Supplementary Information

Interfacial contact between the Cr mask and the SiO_2 substrate

The cross-sectional SEM image (Fig. S1) reveals a continuous and intimate interface between the Cr mask and the SiO_2 substrate, with no observable interfacial gaps or delamination. This confirms that the mask-substrate contact is well maintained during processing. Such conformal adhesion ensures that the etching front is well defined by the mask edge, without unintended penetration of the etchant along the interface. Consistently, no discernible undercut was observed in any of the samples throughout the experiments.

These observations indicate that mask adhesion does not play a measurable role in influencing the etching kinetics or the resulting etch profiles in this study.

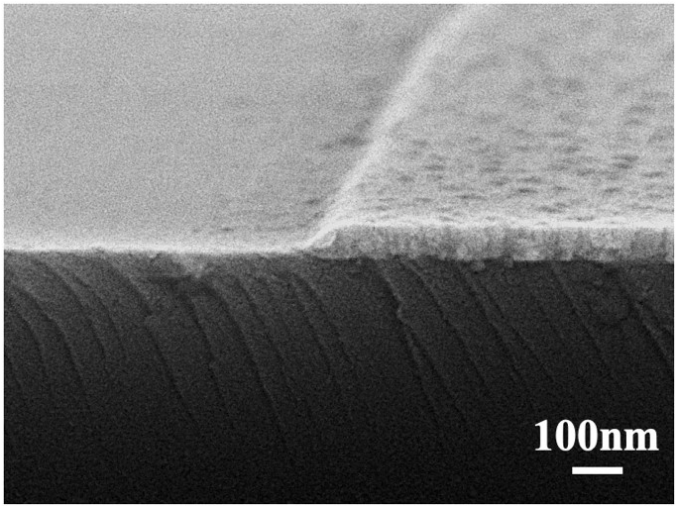

Fig. S1 Cross-sectional SEM image showing the interface between the Cr mask and the SiO_2 substrate.

Explanation of the temperature-dependent suppression of lateral etching

Although BOE etching of SiO_2 is generally regarded as isotropic, reducing the temperature introduces a pronounced anisotropy by preferentially suppressing lateral etching. This behavior originates from the distinct kinetic and mass-transport characteristics of the vertical and lateral pathways.

The etching process can be decomposed into two contributions: vertical etching of the exposed SiO_2 surface and lateral etching propagating beneath the mask. Vertical etching occurs at

an open surface, where fresh etchant is more readily supplied and reaction products are more easily removed. By contrast, lateral etching proceeds within a confined under-mask region, where reagent supply is restricted and reaction products are removed less efficiently. Consequently, the observed lateral etch rate reflects a coupled process involving both interfacial reaction and transport in a confined geometry, making it more temperature-sensitive than vertical etching. As the temperature decreases, this lateral pathway is therefore suppressed more strongly.

The temperature dependence of the rate constant k can be described by the Arrhenius relation (eq. 1):

$$k = Ae^{-\frac{E_a}{RT}} \#(1)$$

where A is the pre-exponential factor related to the frequency of effective collisions, E_a is the apparent activation energy of the overall etching process, R is the universal gas constant, and T is the absolute temperature. As the temperature decreases, reaction pathways associated with higher E_a are exponentially suppressed, leading to a stronger reduction in the lateral etch rate compared with the vertical one.

In addition to kinetic effects, mass transport further amplifies this asymmetry. Beneath the mask, lateral etching is predominantly diffusion-controlled along the interface rather than convection-driven. The diffusion coefficient follows the Stokes-Einstein relation (eq. 2):

$$D = \frac{k_B T}{6\pi\eta r} \#(2)$$

where D is the diffusion coefficient, k_B is the Boltzmann constant, η is the dynamic viscosity of the solution, and r is the hydrodynamic radius of the diffusing species. A decrease in temperature reduces D both directly through the proportional dependence on T and indirectly through the increase in viscosity. Within the confined lateral channel, this reduction in diffusivity intensifies concentration polarization and limits the replenishment of reactive species at the advancing etch front, thereby further hindering lateral propagation.

Taken together, the enhanced temperature sensitivity of the lateral pathway, arising from the coupled effects of interfacial reaction and restricted mass transport, accounts for the anisotropic etching behavior observed at reduced temperature. This interpretation is consistent with the experimentally observed decrease in etch angle and increase in the vertical-to-lateral etch rate ratio.

Quantitative evaluation of etch anisotropy under different conditions

In this study, etch anisotropy was quantitatively extracted from SEM cross-sectional images. Two complementary metrics were employed to characterize the etching profile: (i) the vertical-to-lateral etch-rate ratio, obtained from independently measured etch rates along the vertical and lateral directions, and (ii) the etch inclination angle (α). α is defined as the angle between the vertical axis and a straight line connecting two characteristic points: (1) the intersection of the etched sidewall profile with a horizontal reference line drawn at half of the total etch depth, and (2) the junction between the metal-mask sidewall and the etched region at the cross-section. This geometric definition enables a consistent and reproducible assessment of sidewall anisotropy across different samples.

For the three representative etching conditions listed in Table I (#2, #4, and #5), anisotropy measurements were performed at more than 20 independent locations for each condition. The mean values and corresponding sample standard deviations were calculated to evaluate the statistical reliability and reproducibility of the measurements. The aggregated results are summarized in Table II. Six representative measurement locations for each condition are selected from the full dataset of over 20 measurements (Fig. S2-S4). The extracted vertical and lateral etch rates, the resulting vertical-to-lateral etch-rate ratios, and the corresponding etch inclination angles are listed (Table S1-S3). The relatively small standard deviations observed across all metrics confirm the consistency of the measurement procedure and the robustness of the statistical analysis.

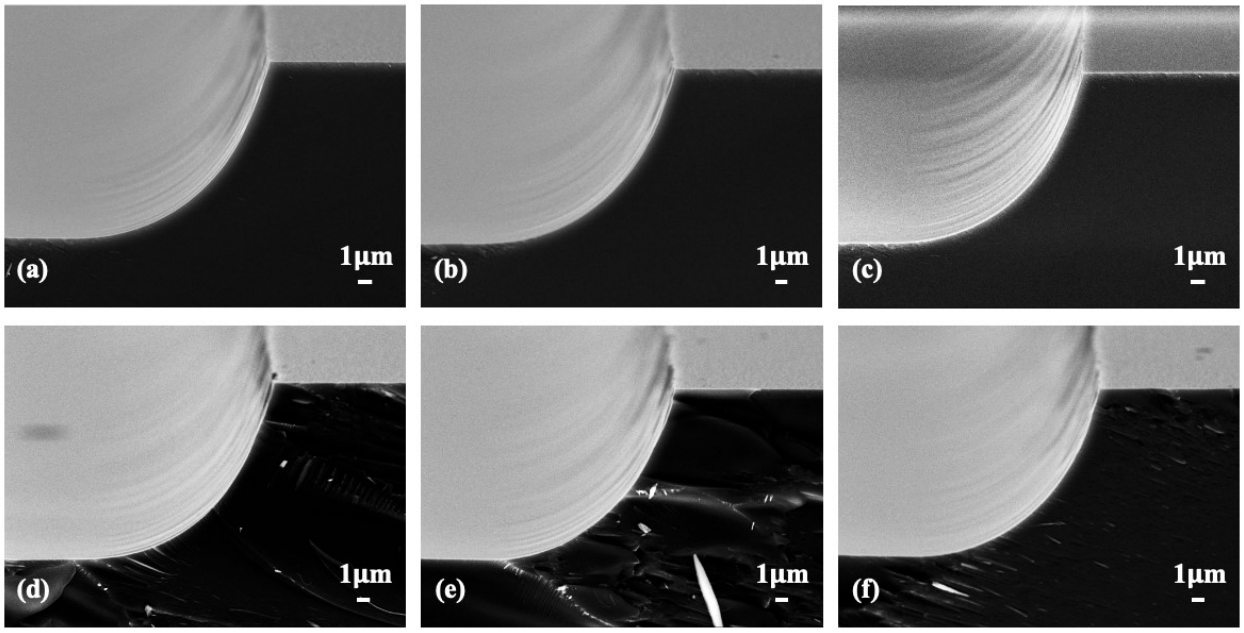

Fig. S2 Cross-sectional SEM images at six representative locations for BOE etching at 25 °C without Triton X-100 addition. (Sample #2)

Table S1. Measurement results corresponding to Fig. S2, including the lateral and vertical etch rates, the vertical-to-lateral etch-rate ratio, and the etch angle.

Location number #	**Lateral etching rate (µm h^{-1})**	**Vertical etching rate (µm h^{-1})**	**Ratio (vertical/lateral)**	**Etch angle α (deg)**
a	5.01	5.87	1.17	21.09
b	5.17	5.77	1.12	21.16
c	5.29	5.60	1.06	22.52
d	5.41	6.11	1.13	20.66
e	5.27	5.96	1.13	22.13
f	5.07	5.76	1.14	21.77
Ave±Dev	5.20 ± 0.15	5.84 ± 0.18	1.12	21.55 ± 0.71

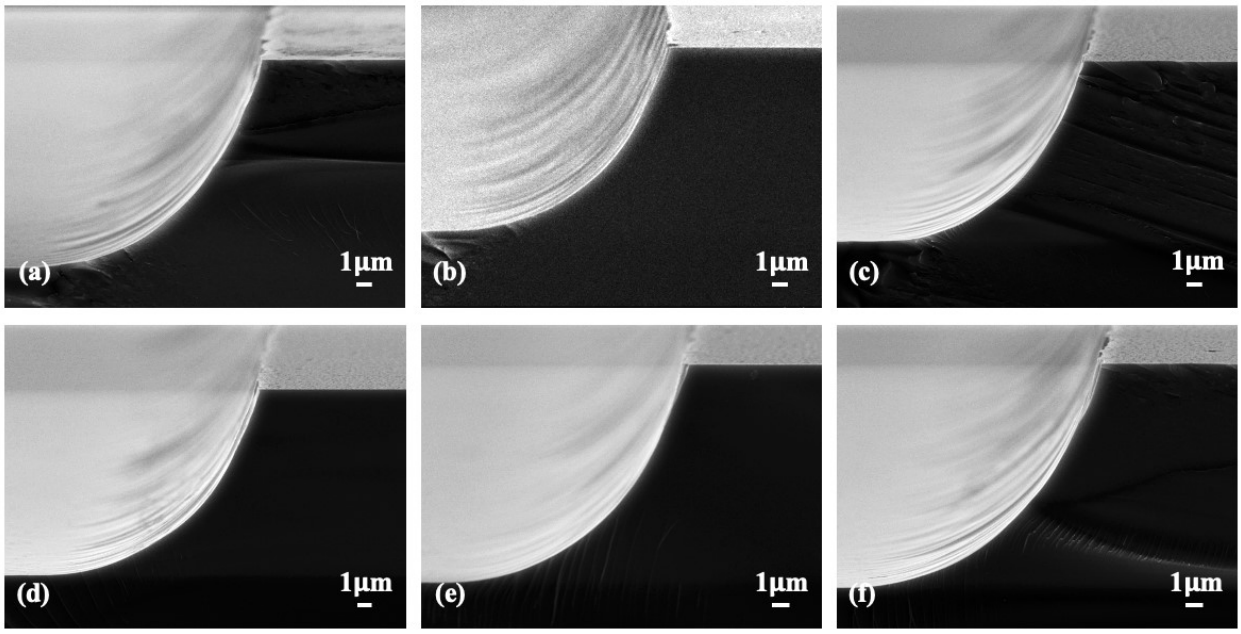

Fig. S3 Cross-sectional SEM images at six representative locations for BOE etching at 25 ℃ with 0.3 mL Triton X-100 addition. (Sample #4)

Table S2. Measurement results corresponding to Fig. S3, including the lateral and vertical etch rates, the vertical-to-lateral etch-rate ratio, and etch angle.

Location number #	**Lateral etching rate (μm h^{-1})**	**Vertical etching rate (μm h^{-1})**	**Ratio (vertical/lateral)**	**Etch angle α (deg)**
a	4.35	5.44	1.25	23.43
b	4.29	5.20	1.21	23.50
c	4.55	5.29	1.16	23.47
d	4.73	5.37	1.14	23.85
e	4.38	5.34	1.22	22.16
f	5.57	5.45	1.19	23.27
Ave±Dev	4.65 ± 0.48	5.35 ± 0.09	1.20	23.28 ± 0.58

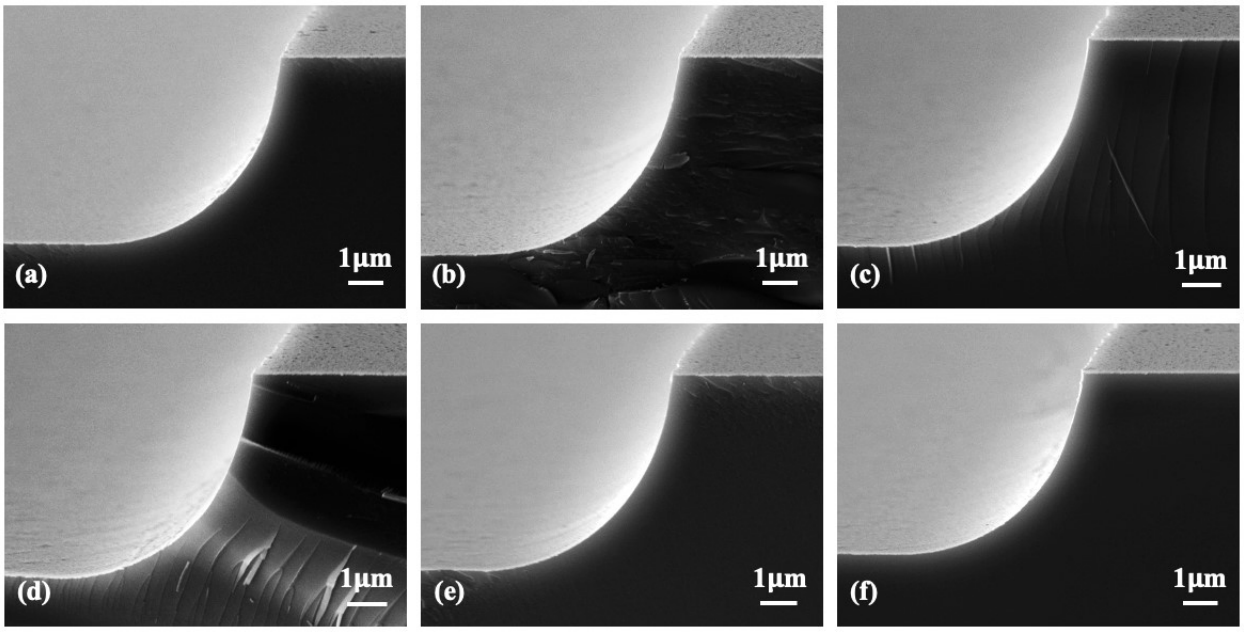

Fig. S4 Cross-sectional SEM images at six representative locations for BOE etching at 0 ℃ with 0.3 mL Triton X-100 addition. (Sample #5)

Table S3. Measurement results corresponding to Fig. S4, including the lateral and vertical etch rates, the vertical-to-lateral etch-rate ratio, and etch angle.

Location number #	**Lateral etching rate (μm h^{-1})**	**Vertical etching rate (μm h^{-1})**	**Ratio (vertical/lateral)**	**Etch angle α (deg)**
a	1.69	2.42	1.43	14.88
b	1.82	2.47	1.36	14.96
c	1.91	2.39	1.25	14.56
d	1.65	2.30	1.40	14.61
e	1.90	2.44	1.28	14.52
f	1.77	2.41	1.36	14.63
Ave±Dev	1.79 ± 0.11	2.40 ± 0.06	1.35	14.69 ± 0.18